Clinical Efficacy and Whole-Exome Sequencing of Liquid Biopsies in a Phase IB/II Study of Bazedoxifene and Palbociclib in Advanced Hormone Receptor–Positive Breast Cancer

Junko Tsuji[1], Tianyu Li[2], Albert Grinshpun[3,4], Tim Coorens[1], Douglas Russo[2,5], Leilani Anderson[3,6], Rebecca Rees[3,6], Agostina Nardone[3,5], Candace Patterson[1], Niall J. Lennon[1], Carrie Cibulskis[1], Ignaty Leshchiner[1], Nabihah Tayob[2,4], Sara M. Tolaney[3,4,6], Nadine Tung[4,7], Donald P. McDonnell[8], Ian E. Krop[3,4,6], Eric P. Winer[3,4,6], Chip Stewart[1], Gad Getz[1,4,9], and Rinath Jeselsohn[3,4,5,6]

ABSTRACT

Purpose: Sensitivity to endocrine therapy (ET) is critical for the clinical benefit from the combination of palbociclib plus ET in hormone receptor–positive/HER2-negative ($HR^+/HER2^-$) advanced breast cancer. Bazedoxifene is a third-generation selective estrogen receptor (ER) modulator and selective ER degrader with activity in preclinical models of endocrine-resistant breast cancer, including models harboring *ESR1* mutations. Clinical trials in healthy women showed that bazedoxifene is well tolerated.

Patients and Methods: We conducted a phase Ib/II study of bazedoxifene plus palbociclib in patients with $HR^+/HER2^-$ advanced breast cancer who progressed on prior ET ($N = 36$; NCT02448771).

Results: The study met its primary endpoint, with a clinical benefit rate of 33.3%, and the safety profile was consistent with what has previously been seen with palbociclib monotherapy. The median progression-free survival (PFS) was 3.6 months [95% confidence interval (CI), 2.0–7.2]. An activating *PIK3CA* mutation at baseline was associated with a shorter PFS (HR = 4.4; 95% CI, 1.5–13; $P = 0.0026$), but activating *ESR1* mutations did not impact the PFS. Longitudinal plasma circulating tumor DNA whole-exome sequencing (WES; $N = 68$ plasma samples) provided an overview of the tumor heterogeneity and the subclonal genetic evolution, and identified actionable mutations acquired during treatment.

Conclusions: The combination of palbociclib and bazedoxifene has clinical efficacy and an acceptable safety profile in a heavily pretreated patient population with advanced $HR^+/HER2^-$ breast cancer. These results merit continued investigation of bazedoxifene in breast cancer.

Introduction

CDK4/6 inhibitors (CDK4/6i) with endocrine therapy (ET) are the standard of care in hormone receptor–positive/HER2-negative ($HR^+/HER2^-$) advanced breast cancer (1). The cyclin D1–dependent kinases CDK4 and CDK6 phosphorylate the pRB tumor suppressor, enabling progression through the cell cycle. Cyclin D1 is a key transcriptional target of the estrogen receptor (ER), and the convergence of the ER transcriptional network and cyclin D1-CDK4/6-Rb1 axis contributes to the synergistic activity of ET and CDK4/6i, such as palbociclib (2–4). This synergy is a key component of the clinical efficacy of palbociclib, which has limited clinical benefit as a single agent (5).

The importance of the synergy between ET and palbociclib suggests that improved targeting of ER may enhance the efficacy of regimens combining ET and palbociclib. This notion is supported by recent studies demonstrating that several mechanisms of resistance to ET are also mechanisms of resistance to the combination of ET and palbociclib (6, 7). Importantly, in the randomized phase III PADA-1 trial, patients with $HR^+/HER2^-$ metastatic breast cancer with an *ESR1*-activating ligand-binding domain (LBD) mutation, which confers resistance to ET, had double the odds of disease progression while on treatment with an aromatase inhibitor (AI) plus palbociclib compared with patients with wild-type (WT) *ESR1* (8). Furthermore, in the PADA-1 trial, patients with rising plasma circulating tumor DNA (ctDNA) *ESR1* mutations had improved progression-free survival (PFS) when treatment was switched to fulvestrant and palbociclib versus continued treatment with an AI and palbociclib (9). In the PALOMA-3 trial, the Y537S *ESR1* LBD mutation was enriched after the acquisition of resistance to fulvestrant alone or to the combination of palbociclib plus fulvestrant in metastatic disease (10). Collectively, these results suggest that better targeting of ER can improve outcomes with the combination of a CDK4/6i and ET, and the Y537S *ESR1* mutation has a role in the acquisition of resistance to fulvestrant and palbociclib.

Bazedoxifene is a selective ER modulator (SERM)-selective ER degrader (SERD) hybrid (SSH; i.e., has ER degrader properties in addition to the SERM activity; refs. 11–13). Bazedoxifene has favorable

[1]Broad Institute of MIT and Harvard, Cambridge, Massachusetts. [2]Department of Data Science, Dana-Farber Cancer Institute, Boston, Massachusetts. [3]Department of Medical Oncology, Dana-Farber Cancer Institute, Boston, Massachusetts. [4]Harvard Medical School, Boston, Massachusetts. [5]Center for Functional Cancer Epigenetics, Dana-Farber Cancer Institute, Boston, Massachusetts. [6]Breast Oncology Program, Dana-Farber Brigham Cancer Center, Boston, Massachusetts. [7]Department of Medical Oncology, Beth Israel Deaconess Medical Center, Boston, Massachusetts. [8]Department of Pharmacology and Cancer Biology, Duke University School of Medicine, Durham, North Carolina. [9]Massachusetts General Hospital Cancer Center and Department of Pathology, Massachusetts General Hospital, Boston, Massachusetts.

Current address for E.P. Winer: Yale Cancer Center, New Haven, Connecticut.

Corresponding Authors: Rinath Jeselsohn, Dana-Farber Cancer Institute, 450 Brookline Avenue, Boston MA 02215 D728. Phone: 617-632-3800; E-mail: rinath_jeselsohn@dfci.harvard.edu; and Gad Getz, gadgetz@broadinstitute.org

Clin Cancer Res 2022;28:5066–78

doi: 10.1158/1078-0432.CCR-22-2305

Translational Relevance

In this clinical trial, we show that bazedoxifene plus palbociclib has clinical efficacy in patients with advanced hormone receptor–positive breast cancer and this combination is well tolerated. Pathogenic *PIK3CA* mutations are a candidate biomarker of resistance to bazedoxifene plus palbociclib. In addition, we demonstrate the utility of circulating tumor DNA whole-exome sequencing and the significance of determining the subclonal evolution in individual patients.

effects on bone and lipid metabolism without adversely affecting the uterus (14, 15). It is the only SERM that is approved in combination with conjugated estrogens for the prevention of postmenopausal symptoms and osteoporosis based on large randomized clinical trials in healthy postmenopausal women (16). Preclinical studies showed that bazedoxifene has antitumor activity in HR^+ breast cancer models, including models of resistance to tamoxifen, resistance to estrogen deprivation, and models harboring a Y537S ER LBD mutation (11, 12, 17, 18). Preclinical studies showed that bazedoxifene had greater inhibitory effects on cell growth and ER-mediated transcription compared with tamoxifen or fulvestrant in the presence of the Y537S *ESR1* mutations (13, 19). Computational predictions and, more recently, the crystal structure of mutant LBD bound to bazedoxifene showed that the Y537S-mutant LBD bound to bazedoxifene leads to the formation of a new S537-E380 hydrogen bond that stabilizes helix 12 (H12) in the activating function-2 (AF-2) cleft of the LBD, and this enables the inhibition of coactivator binding that results in transcriptional inhibition. In contrast, several other SERMS and SERDs, including tamoxifen and fulvestrant, were shown to have limited transcriptional inhibitory activity in the presence of the Y537S mutation. This is likely because H12 is pushed out from the AF-2 cleft of the Y537S-mutant LBD after interacting with tamoxifen or fulvestrant, and this allows coactivator binding and consequently a decreased response to these drugs (13, 19).

Taken together, based on the preclinical data of bazedoxifene in endocrine-resistant HR^+ breast cancer models, the safety profile of bazedoxifene in randomized clinical trials, and the rationale of combining palbociclib with next-generation ETs, we conducted the first clinical trial with the combination of palbociclib and bazedoxifene. This was a phase Ib/II study designed to investigate the efficacy and safety of palbociclib with bazedoxifene for the treatment of patients with HR^+/$HER2^-$ advanced breast cancer who had progressed on prior ET. In addition, we performed serial ctDNA whole-exome sequencing (WES) to study genetic mechanisms of resistance and the tumor clonal architecture and evolution during treatment with palbociclib and bazedoxifene.

Patients and Methods

Patient population

We enrolled female or male patients ages 18 years or older with histologically confirmed invasive breast cancer that was metastatic or unresectable locally advanced disease. Primary or invasive disease was confirmed to be HR^+ (ER >10% and/or progesterone receptor>10%) and $HER2^-$ according the American Society of Clinical Oncology/College of Pathology guidelines (20) [defined as 0–1+ by IHC or FISH-negative (HER2 copy number < 6 and HER2/CEP17 ratio < 2.0)]. Measurable disease was required per RECIST 1.1 (21). Bone-only disease was allowed if there was evidence of lytic lesions (22). Progressive disease on prior ET was required; this was defined as relapse while on adjuvant ET or within 1 year of completion of adjuvant ET, or progression through at least one line of ET in metastatic or locally advanced breast cancer. Postmenopausal and premenopausal women who have been on a GnRH agonist were eligible. Prior treatment with up to two lines of chemotherapy in advanced disease was allowed. The protocol was amended to allow up to one line of prior chemotherapy when the 18th patient was enrolled. There was no limit to the number of prior endocrine therapies.

Study design and treatment

The study was a phase IB/II, single-arm, single-institution, and open-label study. The objectives were to evaluate the safety and antitumor activity of the combination of palbociclib and bazedoxifene. The primary endpoint was clinical benefit rate (CBR), defined as the proportion of patients with complete response (CR), partial response (PR), or stable disease (SD) at week 24 [per RECIST version 1.1 (21)]. A CBR of 20% or less would not be of clinical interest based on a conservative estimate of the percentage of patients who progressed on adjuvant ET or progressed on ET or palbociclib as a single agent in metastatic disease (5). Secondary endpoints included objective response rate, PFS, overall survival (OS), and safety. Objectives were determined in the intention-to-treat (ITT) population and the evaluable cohort who reached the first restaging timepoint.

All patients received bazedoxifene 40 mg orally once daily on days 1–28 and palbociclib 125 mg orally once daily on days 1–21 of a 28-day cycle. The bazedoxifene dose of 40 mg was based on published safety data for this dose (23). The first 6 patients enrolled completed a safety run-in, and accrual was paused for safety assessment after these patients completed at least one treatment cycle. Response and progression were evaluated using RECIST 1.1 guidelines (21). For patients with bone-only disease, evaluation was done per MD Anderson bone tumor response criteria (22). After a baseline scan, tumor response was assessed every 8 weeks, with a PR or CR requiring confirmation within 4–6 weeks. After cycle 6, tumor measurements were performed every 12 weeks. Safety was evaluated according to NCI-CTCAE version 4.0. Exploratory translational objectives were to investigate the efficacy of the combination of bazedoxifene and palbociclib in relation to genomic findings in ctDNA.

Statistical analyses

The study followed a Simon "optimal" two-stage design. On the basis of the published activity of palbociclib as a single agent, a CBR of 20% or less was considered not to be of clinical interest and was the null hypothesis, and a CBR of ≥ 30% was considered worthy of further investigation. The sample size of 37 patients was chosen to have 90% power to declare the combination effective at this rate while controlling for no more than 10% one-sided type I error under the null hypothesis. The first stage of the study included 17 evaluable patients, and accrual was continued to the second stage after the confirmation that at least 4 patients met the primary endpoint.

CBR was reported as a proportion and 95% confidence interval (CI) accounting for the two-stage design. Associations between CBR and clinical and/or correlative factors were assessed using the Wilcoxon test for continuous variables and Fisher exact test for categorical variables.

Median PFS in months was estimated using the Kaplan–Meier estimation method and compared between clinical and/or correlative factors via log-rank test. HRs were obtained using Cox proportional

hazards models. All tests were two sided with a type I error of 0.05. All analyses were carried out via SAS, V9.4 (SAS Institute) and R, V4.0.2.

Sample collection and processing

Whole venous blood (6–10 mL) was collected from patients into ethylenediaminetetraacetic acid vacutainer tubes (Becton and Dickinson). Blood was processed within 2 hours of collection. Whole blood was centrifuged for 10 minutes at 1,200 × *g* and the plasma supernatant was cleared by centrifugation for 10 minutes at 3,000 × *g*. Cell-free DNA (cfDNA was extracted from 2 to 7 mL of plasma and eluted into 40–80 μL of resuspension buffer using the Qiagen Circulating DNA kit on the QIAsymphony liquid handling system. Germline DNA (gDNA) was extracted using the Qiasymphony DSP DNA midi kit on the QIAsymphony liquid handling system. Quantification of extracted cfDNA and gDNA was performed using the PicoGreen (Life Technologies) assay on a Hamilton STAR-line liquid handling system. Library preparation was performed using a commercially available kit (KAPA HyperPrep Kit with Library Amplification product KK8504) and IDT's duplex UMI adapters. Unique 8-base dual index sequences embedded within the p5 and p7 primers (purchased from IDT) were added during PCR. Enzymatic clean-up was performed using Beckman Coultier AMPure XP beads. Samples were sequenced using Illumina sequencing technology.

ctDNA analysis

Sequenced reads in both ultra-low passage whole-genome sequencing (ULP-WGS) and WES libraries were mapped to the human reference genome (hg19) with BWA-MEM (version 0.17.7; RRID: SCR_010910). PCR duplicates were flagged by MarkDuplicates in Picard tool (version 2.26.10; RRID: SCR_006525). ichorCNA (version 0.1; ref. 24) was run for estimating tumor purity estimation. We applied the hg19 panel of normals provided in the ichorCNA github repo (inst/extdata/HD_ULP_PoN_1Mb_median _normAutosome_-mapScoreFiltered_median.rds).

SNV/indel detection

Somatic mutations on the exome data were called by The Cancer Genome Analysis (TCGA) WES Characterization Pipeline (the CGA pipeline). The CGA pipeline first runs deTiN (25) and ContEst (ref. 26; RRID: SCR_000595) for estimating potential tumor-in-normal contamination and cross-patient contamination, and calls single-nucleotide variants (SNV) and indels with MuTect (ref. 27; RRID: SCR_000559) and Strelka (ref. 28; RRID: SCR_005109), respectively. Out of the 68 exome samples, two samples were processed as tumor-only due to lack of the matched normals. For the tumor-only runs, CalculateContamination in GATK4 (version 4.0.5.1; RRID: SCR_001876) was used for estimating the cross-patient contamination. For the indel calling step in the tumor-only runs, an unmatched normal sample was used for Strelka, which requires a matched normal input. Potential artifacts were filtered with two panels of normals (created from 298 normal samples and 8,334 TCGA normal samples, respectively), the BLAT (RRID: SCR_011919) read-realignment filter, and the read orientation bias filters. The mutations in the tumor-only runs were further filtered if the called mutations overlapped with the germline mutations with the population allele frequencies ≥5% in the gnomAD database (ref. 29; RRID: SCR_014964). Mutations were denoted as pathogenic or likely pathogenic based on OncoKB (ref. 30; RRID: SCR_014782).

Mutational signatures were extracted using two algorithms: (i) hierarchical Dirichlet process (HDP; https://github.com/nicolaroberts/hdp) based on the Bayesian hierarchical Dirichlet process, and (ii) SignatureAnalyzer based on Bayesian non-negative matrix factorization (31). The Gibbs sampler was run with 20,000 burn-in iterations (parameter "burnin"). With a spacing of 200 iterations (parameter "space"), 100 iterations were collected (parameter "*n*"). After each Gibbs sampling iteration, three iterations of concentration parameter sampling were performed (parameter "cpiter"). To deconvolute composite signatures and to equate obtained HDP signatures to reference signatures, we used an expectation-maximization algorithm to deconstruct these signatures into reference constituents (31). Because of the low burden of indels, we excluded a mismatch repair deficiency signature (SBS6) and homologous repair deficiency signature (SBS3) from the candidate list using SigFit (32).

Copy-number alterations in the WES samples were detected by GATK-CNV (version 4.1.2.0; RRID: SCR_001876) with -number-of-changepoints-penalty-factor = 2.0. As the postfiltering steps, a panel of normals created from 298 normal samples was used, and potential germline copy-number alterations were discarded. The allelic copy-number alteration outputs from ModelSegments in GATK-CNV (version 4.1.2.0) were used for estimating tumor purity with ABSOLUTE (ref. 33; RRID: SCR_005198). The estimated tumor purity between the exomes (ABSOLUTE) and the ULP-WGS data (ichorCNA) was highly correlated (Pearson correlation coefficient = 0.98). Tumor mutation burden (TMB) was calculated as the number of coding mutations per Mb of covered exons.

The genomic sites of detected mutations across serial WES in a patient were force-called by investigating the number of reference and alternate bases at the sites. Somatic copy-number alterations (SCNA) in the serial WES were also grouped across the timepoints. PhylogicNDT was run with 500 iterations of Markov chain Monte Carlo Gibbs sampler on the force-called mutations and SCNAs to assign mutations to clonal clusters for estimating the phylogeny (34).

Compliance with ethical standards

The study was conducted in accordance with the International Conference on Harmonization Good Clinical Practice Standards and the Declaration of Helsinki. Institutional review board approval was obtained at Dana-Farber/Harvard Cancer Center (DF/HCC). The study was registered in ClinicalTrials.gov (NCT02448771). The DF/HCC Data and Safety Monitoring Committee, which is composed of clinical specialists with experience in oncology and who had no direct relationship with the study, reviewed and monitored toxicity and accrual data from the study. Participants provided written informed consent prior to the performance of any protocol specific procedures or assessments. The study was an investigator-initiated trial funded by Pfizer. Palbociclib and bazedoxifene were supplied by the manufacturer (Pfizer). The funder had no role in data collection, data analysis, or data interpretation.

Data and materials availability

TCGA pan-cancer data are available through a data portal (https://gdc.cancer.gov/node/905/; https://gdc.cancer.gov/about-data/publications/pancanatlas). The WES data from this study was deposited in dbGap accession number phs002802.v1.p1.

Results

Patients

Between July 2015 and July 2017, we enrolled 36 patients with advanced $HR^+/HER2^-$ breast cancer (34 females and 2 males; Supplementary Fig. S1). The study met its primary endpoint after enrolling 36 patients. Patient demographics and baseline characteristics are in **Table 1** and Supplementary Table S1 (Supplementary Table S1

Table 1. Baseline characteristics of study participants in the intention-to-treat patient population.

Characteristic	Number of patients (%)
Sex	
Male	2 (6%)
Female	34 (94%)
ECOG performance status	
00	33 (92%)
01	3 (8%)
Estrogen receptor status	
Low positive	1 (3%)
Positive (>10%)	35 (97%)
Progesterone receptor status	
Unknown	1 (3%)
Low positive	1 (3%)
Positive (>10%)	22 (61%)
Negative (≤10%)	12 (33%)
HER2 status	
Negative	36 (100%)
Sites of disease	
Lymph nodes	13 (36%)
Breast and chest wall	14 (39%)
Lung	12 (33%)
Liver	23 (64%)
Bone	26 (72%)
Other	7 (19%)
Bone only	
Yes	2 (6%)
No	34 (94%)
Visceral disease	
Yes	29 (81%)
No	7 (19%)
Prior lines of hormonal treatment for metastatic breast cancer	
0	6 (17%)
1	12 (33%)
2	7 (19%)
3	8 (22%)
4	2 (6%)
5	1 (3%)
Prior lines of chemotherapy for metastatic breast cancer	
0	17 (47%)
1	16 (44%)
2	3 (8%)
Everolimus for metastatic breast cancer	
Yes	4 (11%)
No	32 (89%)

Abbreviation: ECOG, Eastern Cooperative Oncology Group.

includes the study representative information). All patients had ER^+, $HER2^-$ disease. The median age was 59.5 years (range, 37–79 years). Most of the patients had liver metastases (64%, 23/36) and 33% of patients (12/36) had lung metastases. Only 6% of patients (2/36) had bone-only disease. All patients had disease progression while on ET or disease recurrence within 1 year of completion of adjuvant ET. Most patients were heavily pretreated, with 50% of patients (18/36) having received two or more prior lines of ET and 52% of patients (19/36) having received up to two lines of chemotherapy in advanced disease. Nearly all patients (28/36) had disease progression while on treatment with an AI or disease recurrence within 1 year of completion of adjuvant treatment with an AI. There were 7 (19%) patients who received prior treatment with fulvestrant and 4 (11%) patients who received prior treatment with everolimus.

Table 2. Adverse events related to study treatment in at least 5% of patients.

Adverse event	All grades (%)	Grade ≥ 3 (%)
Neutrophil count decreased	22 (61.1%)	17 (47.2%)
Fatigue	8 (22.2%)	0 (0%)
Anemia	3 (8.3%)	1 (2.8%)
Mucositis oral	3 (8.3%)	0 (0%%)
White blood cell decreased	3 (8.3%)	1 (2.8%)
Gastroesophageal reflux disease	2 (5.6%)	0 (0%)
Thrombocytopenia	2 (5.6%)	1 (2.8%)

Treatment administration and safety

At the data cutoff in August 2020, with a median follow-up of 29.6 months, all patients had discontinued palbociclib and bazedoxifene treatment. A median of 4 cycles were given per patient (range, 1–34). The first 6 patients who were included in the safety run-in did not experience any dose-limiting toxicities (DLT) during their first treatment cycle. Thus, all patients were given 125 mg palbociclib for the remainder of the study. Neutropenia (61%) and fatigue (22%) were the most common adverse events associated with study treatment. A total of 16 patients (44%) experienced grade 3 neutropenia, and 1 patient (3%) experienced grade 4 neutropenia (**Table 2**; Supplementary Table S2). There were no deaths attributed to the study treatment. Most patients discontinued treatment due to disease progression (83%). Only 1 patient (3%) discontinued treatment due to protocol-specified unacceptable toxicity (neutropenia). Palbociclib dose reductions were required in 14 (38.9%) patients due to toxicity. Doses were held in 23 (63.9%) patients for a median of 10 days (range, 1–45 days). There were no bazedoxifene dose reductions, and bazedoxifene doses were held in 13 (36.1%) patients for a median of 12 days (range, 5–22 days; Supplementary Tables S3 and S4).

Efficacy

Of the 36 patients, 1 patient was unevaluable (this patient developed grade 4 neutropenia during the first cycle) and was included in the ITT analysis (**Table 3**). In the first stage of the study, 17 evaluable patients

Table 3. Summary of efficacy in ITT and evaluable patients.

Response	Intention-to-treat cohort ($n = 36$)	Evaluable cohort ($n = 35$)
Best overall response *n* (%)		
Complete response (CR)	0 (0%)	0 (0%)
Partial response (PR)		
Total	4 (11.1%)	4 (11.4%)
Confirmed	1 (2.8%)	1 (2.9%)
Unconfirmed	3 (8.3%)	3 (8.6%)
Stable disease (SD)	20[a] (55.6%)	20 (57.1%)
SD ≥ 24 weeks	11 (30.6%)	11 (31.4%)
Progressive disease	14 (38.9%)	14 (40%)
Clinical benefit rate (CR + PR + SD ≥ 24 weeks)	12 (33.3%)	12 (34.3%)
Response duration ≥ 12 months	4 (11.1%)	4 (11.5%)
Median PFS, months (95% CI)	3.6 (2–7.2)	
Median OS, months (95% CI)	26.5 (20.7-NA)	

Abbreviations: CI, confidence interval; OS, overall survival; PFS, progression-free survival.

[a]Includes the 3 unconfirmed PR patients. They all had SD ≥ 24weeks.

were enrolled; 5 of these patients achieved a clinical benefit (SD ≥ 24 weeks). The study continued to the second stage and accrued 19 additional patients. Accounting for the two-stage design, the best overall response in the ITT analysis was SD in 20 patients (20/36, 55.6%), progressive disease in 14 patients (14/36, 38.9%) and a confirmed PR in 1 patient. Among the patients with SD, 3 patients had unconfirmed PR (**Fig. 1A**). The CBR at ≥ 24 weeks was 33.3% (12/36; 95% CI, 9.8–56.4) accounting for two-stage design. This exceeded the predetermined boundary of at least 11 patients experiencing clinical benefit and therefore met the primary endpoint. These included 1 patient with a confirmed PR and 11 patients with SD ≥ 24 weeks. When including only evaluable patients, the CBR at ≥ 24 weeks was 34.3% (12/35; 95% CI, 20.7–58.9) accounting for two-stage design. Of the patients who achieved a clinical benefit at ≥ 24 weeks, 4 patients (4/36, 11.1%) had an exceptional clinical benefit with disease stability for ≥ 12 months (**Fig. 1A** and **B**; **Table 3**). The median PFS was 3.6 months (95% CI, 2.0–7.2; **Fig. 1C**), and the median OS was 26.5 months (95% CI, 20.7–not reached; **Fig. 1D**). There was no association between prior treatment regimens in the metastatic setting and the clinical benefit, including; prior tamoxifen treatment [prior tamoxifen, 30.8% (8/26) vs. no prior tamoxifen, 40% (4/10); $P = 0.7$, Fisher exact test for all comparisons in this section], prior fulvestrant [prior fulvestrant, 28.6% (2/7) vs. no prior fulvestrant, 34.5% (10/29); $P = 0.8$], or prior chemotherapy treatment [prior chemotherapy, 36.8% (7/19) vs. no prior chemotherapy, 29.4% (5/17); $P = 0.7$]. There was also no association between the number of prior treatment regimens in the metastatic setting and clinical benefit [0–1 lines of treatment, 33.3% (3/9) vs. ≥ 2 lines of treatment, 33.3% (9/27); $P = 1.0$]. However, liver metastases versus no liver metastases [17.4% (4/23) vs. 61.5% (8/13), respectively], or three to four organs with metastatic involvement versus two organs versus one organ with metastatic involvement [14.2% (3/21) vs. 60% (6/10) vs. 60% (3/5), respectively] were associated with decreased clinical benefit ($P = 0.01$).

Cell-free DNA tumor fraction dynamics

Plasma samples were collected at baseline ($n = 36$), day 1 of cycle 2 (C2D1; $n = 33$) and at the time of disease progression at the end of treatment (EOT; $n = 33$) to identify genetic alterations associated with primary or acquired resistance to bazedoxifene and palbociclib (Supplementary Fig. S2A and S2B). All samples ($n = 102$) were subjected to ULP-WGS (mean coverage 0.19–0.57X) to determine cell-free DNA (cfDNA) tumor fraction (TF; see Patients and Methods) for the selection of samples with detectable ctDNA for subsequent WES, and to determine the relationship between the TF and clinical outcomes (Supplementary Fig. S3A). The median tumor fraction in all samples was 0.04 [range (0–0.85)]. Baseline cfDNA TF was higher in patients with liver metastases [median = 0.07 (0–0.85)] versus patients without liver metastases [median = 0.04 (0–0.3)] (Wilcoxon $P = 0.01$; Supplementary Fig. S3B) and patients who had three to four organs involved with metastases [median = 0.06 (0–0.85)] versus one organ involved with metastases [median = 0.03 (0–0.04)] (Wilcoxon $P = 0.03$). Moreover, baseline cfDNA TF correlated with PFS; patients with a high baseline cfDNA TF (≥0.1) had a lower PFS ($n = 12$, median PFS = 1.94 months) compared with patients with a low cfDNA TF (<0.1; $n = 24$, median PFS = 5.56 months; HR = 2.29; 95% CI, 1.08–4.89; $P = 0.027$, log-rank test; Supplementary Fig. S3C). There was no significant association between the changes in cfDNA TF after 1 month of treatment and PFS [ratio between C2D1/baseline TF > 1 ($n = 12$), median PFS = 2.04 months; vs. C2D1/baseline TF ≤1 ($n = 19$), median PFS = 3.67 months, HR = 0.9; 95% CI, 0.4–1.9; $P = 0.71$] (Supplementary Fig. S3D). Comparison of the TF at C2D1 and the EOT showed an increase in TF in most cases (58%, 18/31). The TF was unchanged in 7 patients (23%) and in 6 patients (19%) there was a decrease at the EOT. In most of the cases in which the TF decreased at the EOT, the absolute change was marginal and the TF either remained low (in the range of 0.03) or very high (above 0.45) except for one patient (patient 25) who had a decrease in the TF from 0.6 at C2D1 to 0.045 at the EOT. This patient had an increase in the size of the liver metastases but a mixed response of bone metastases with evidence of decreased fluorodeoxyglucose uptake in several bone metastases based on a PET-CT scan. Thus, although the early cfDNA TF dynamics were not indicative of PFS, the cfDNA TF was overall reflective of metastatic burden and in most cases of disease progression.

Genomic alterations and clinical benefit

Samples with detectable ctDNA (cfDNA TF > 0.03) were subjected to WES (mean target coverage = 90–461X, median = 193X). WES was performed in 68 samples [baseline 28/36 (78%), C2D1 19/34 (56%) and EOT 23/32 (78%)] (Mutation Annotation Format in Supplementary table S5). These included 20 matched pairs of baseline and EOT samples. Sample-to-sample correlation of the somatic SNVs (SSNV) in the 68 samples showed that the matched samples from an individual patient had the strongest correlation in nearly all cases except for two samples that had a low number of mutations (Supplementary Fig. S4A). As expected, most of the SSNVs in exonic regions were unique to a single patient (4,205 of 4,227 nonsilent SSNVs, 99.5%; 3,190 of 3,211 silent SSNVs, 99.3%). The most frequent SSNVs were oncogenic hotspot mutations in *ESR1* and *PIK3CA* (Supplementary Fig. S4B).

We next focused on known cancer-related genes (list of genes and the detected amino acid changes in Supplementary Table S6). At baseline, the most frequent mutations in the cancer-related genes included pathogenic or likely-pathogenic mutations in *ESR1* (**Fig. 2B**), pathogenic *PIK3CA* mutations (**Fig. 2D**), *EPAS1* (none of these are known to be pathogenic) and *TP53* mutations (Supplementary Table S6). Other baseline pathogenic or likely pathogenic mutations identified in at least 2 patients included *AKT1* and *KMT2C* mutations (**Figs. 2A–C**; Supplementary Table S6). Pathogenic *ESR1* mutations were found in 32% (9/28) of baseline samples, with the missense mutations Y537 and D538 accounting for the majority of the *ESR1* mutations (**Fig. 2B**). *ESR1* mutations were detected in patients who had or did not have a clinical benefit at ≥ 24 weeks (**Fig. 2A**), and there was no association between the *ESR1* mutations and PFS [WT median PFS = 3.6 months ($n = 19$), mutant median PFS = 2.0 months ($n = 9$); HR = 1.0; 95% CI, 0.4–2.4; $P = 0.94$, log-rank test for all comparisons in this section] (**Fig. 2D**). In contrast, baseline hotspot *PIK3CA* mutations were not detected in patients who had a clinical benefit at ≥ 24 weeks (**Fig. 2A**), and patients with a baseline *PIK3CA* mutation had a lower PFS compared with patients with WT *PIK3CA* at baseline [WT median PFS = 3.9 months ($n = 22$), mutant median PFS = 1.8 months ($n = 6$); HR = 0.2; 95% CI, 0.06–0.6, $P = 0.0019$] (**Fig. 2E**). This difference remained significant in a multivariate analysis correcting for significant clinical variables including the presence of liver metastases versus no liver metastases and 1 versus three to four organs with metastases (mutant vs. WT HR = 3.82; 95% CI, 1.18–12.33; $P = 0.025$; Supplementary Table S7). In addition, patients who had a baseline truncating mutation, including mostly pathogenic or likely pathogenic mutations in tumor suppressor genes (*TP53, MEN1, RB1, CDKN1B, NF1, TP53, BP1, TP63, SMAD2, SMAD4, ARID1A*, and *KMT2C*), had a worse PFS in a univariate analysis [no truncating mutation PFS = 3.8 months ($n = 21$), truncating mutation median PFS = 1.7 months ($n = 7$), HR = 0.3; 95% CI, 0.1–0.7; $P = 0.006$] and in a

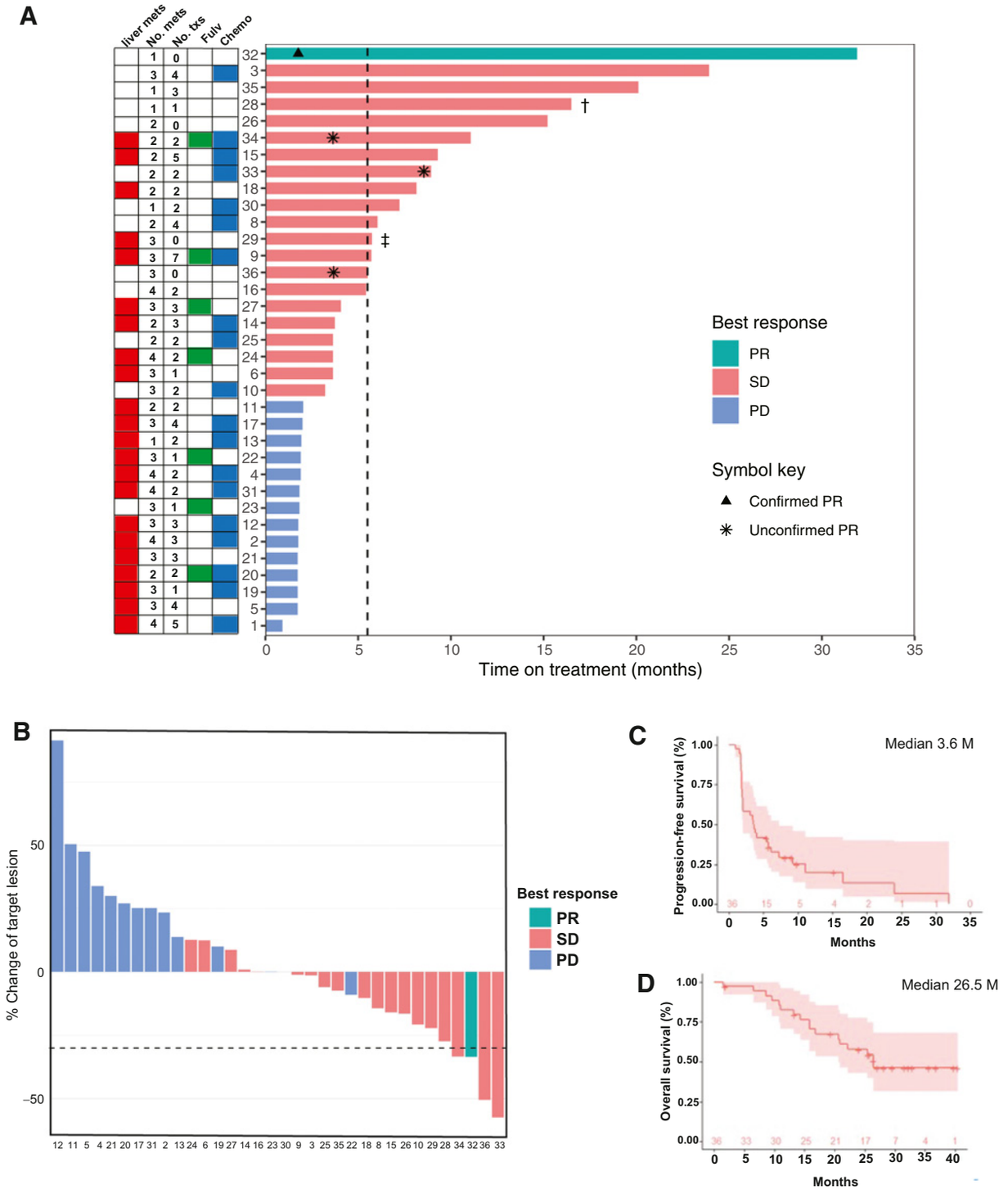

Figure 1.

Efficacy of bazedoxifene and palbociclib in evaluable patients. **A,** Swimmer plot of 34 patients evaluable for time to event endpoints. Vertical dotted line indicates 6 months. The left panel denotes patients who have liver metastases (liver mets) in red, the number of organs involved with metastases (number of mets), number of lines of treatment in the metastatic setting (patients who had not received treatment in metastatic disease developed disease recurrence during or within 1 year of adjuvant ET), prior fulvestrant (Fulv) treatment indicated in green, and prior chemotherapy treatment indicated in blue (Chemo). †Patient 28 stayed on treatment for 18 cycles despite the PD assessment after cycle 2. ‡Patient 29 stayed on treatment for an additional 14 days after the last disease evaluation. Neither patient 28 nor patient 29 is considered as having clinical benefit. **B,** Waterfall plot with best percentage of tumor changes from baseline sum of the longest diameter in target lesions of the 34 evaluable patients. Response is based on RECIST 1.1. Horizontal dotted line indicates −30% change of targeted lesion. **C,** Kaplan–Meier curve representing PFS for ITT patient population ($n = 36$). Median PFS, 3.6 months; 95% CI: 2–7.2 months. **D,** Kaplan–Meier curve representing OS for the ITT patient population ($n = 36$). Median OS, 26.5 months (95% lower confidence limit, 20.7 months). PD, progressive disease; PR, partial response; SD, stable disease.

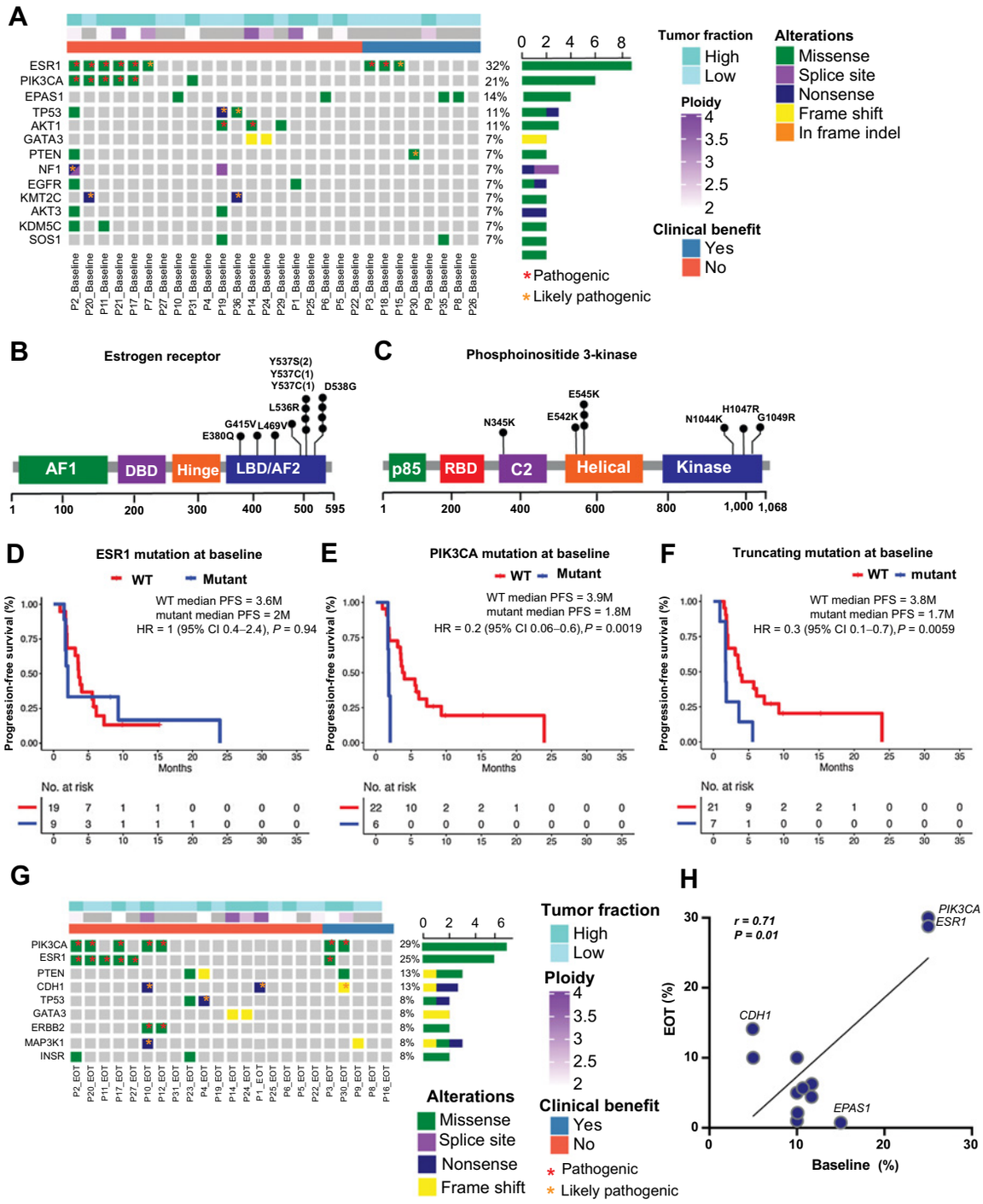

Figure 2.

WES. **A,** Baseline somatic mutations in cancer-related genes detected by ctDNA WES ($n = 28$) in at least 2 patients. **B,** Lollipop diagram denoting the *ESR1* mutations detected in the baseline ctDNA samples. **C,** Lollipop diagram denoting the *PIK3CA* mutations detected in the baseline ctDNA samples. **D,** Kaplan–Meier curve representing PFS during treatment with palbociclib and bazedoxifene in patients with baseline ctDNA WES stratified by no/yes baseline *ESR1* ctDNA mutation. The median PFS for patients with WT *ESR1* versus mutant *ESR1* is 3.6 months and 2 months, respectively. HR = 1.0 (95% CI: 0.4–2.4); $P = 0.94$, log-rank test. **E,** Kaplan–Meier curve representing PFS on treatment for patients with baseline WES ctDNA analysis stratified by no/yes baseline ctDNA *PIK3CA* mutation. The median PFS for patients with WT *PIK3CA* versus mutant *PIK3CA* was 3.9 months versus 1.8 months, respectively. HR = 0.2 (95% CI: 0.06–0.6); $P = 0.0019$, log-rank test. **F,** Kaplan–Meier curve representing PFS on treatment for patients with baseline WES ctDNA analysis stratified by no/yes baseline ctDNA truncating mutation. The median PFS for patients without a truncating mutation versus with a truncating mutation was 3.8 months versus 1.7 months, respectively. HR = 0.3 (95% CI: 0.1–0.7); $P = 0.0059$, log-rank test. **G,** EOT somatic mutations in cancer-related genes detected by ctDNA WES ($n = 22$) in at least 2 patients. **H,** Correlation of the frequency of mutations in cancer-related genes that were detected in at least 2 patients and including patients with matched baseline and EOT treatment ctDNA WES ($n = 20$), $r = 0.7$, $P = 0.01$, Pearson correlation. ctDNA, circulating tumor DNA.

multivariate analysis (mutant vs. WT HR = 3.01; 95% CI, 1.09–8.3; $P = 0.034$; **Fig. 2F**; Supplementary Table S7).

Consistent with the baseline ctDNA, the most common SSNVs in cancer-related genes at the EOT were *PIK3CA* (32%, 7/22) and *ESR1* (27%, 6/22), followed by *PTEN*, *TP53*, and *GATA3* (**Fig. 2G**). Comparison of the matched baseline and EOT ctDNA pairs showed a high correlation between the frequency of the mutations found in at least two different patients ($r = 0.7$, $P = 0.01$, Pearson correlation; **Fig. 2H**). However, when comparing EOT ctDNA versus baseline ctDNA in individual patients, several patients gained actionable driver mutations at the EOT that are suggestive of putative mechanisms of acquired resistance and offer potential therapeutic targets. As examples, one patient (patient 30) who was on treatment for 7 months gained two *BRAF* missense mutations (G469A and D287H) and 2 hotspot *PIK3CA* mutations (E365K and N1044K). A second patient (patient 10) was on treatment for 3 months and gained pathogenic mutations in *ERBB2* (S310Y) and *PIK3CA* (H1047L), and a missense mutation in *FGFR2* (L309V; Supplementary Fig. S5).

SCNA analysis was performed in 30 plasma ctDNA samples from 16 patients with a TF ≥ 0.15 (baseline $n = 12$, C2D1 $n = 9$, EOT $n = 9$; **Fig. 3A**). Two patients (patient 1 and patient 14) were found to have genome doubling, which is associated with poor outcomes (35). In all samples, there were SCNAs in at least two cancer-related driver genes. In addition, in all samples we identified SCNAs in at least one gene related to a potential mechanism of resistance to ET and/or CDK4/6i. These included SCNAs in *CCND1, CCNE2, MYC, ESR1, CDKN2B, CDKN2A, FOXA1, PIK3CA, AURKA, AURKB, CDKN1A, FGFR1, CDK6, CDK4, IGF1R*, or *PTEN* (7, 36–38). Amplifications or gains in *CCND1* and other genes that are within the same genomic region on 11q13.3 (*FGF19, FGF3*, and *FGF4)* were among the most common SCNAs. In addition, *ELF3* amplifications or gains were identified in most of the patients (69%, 11/16). In line with the high frequency of *ELF3* SCNAs that we identified, amplifications of *ELF3* are more frequent in $ER^+/HER2^-$ metastatic breast cancers in the Metastatic Breast Cancer Project (39, 40) versus the $ER^+/HER2^-$ primary breast cancers in TCGA cohort (ref. 41; 31%, 22/70 in metastatic tumors vs. 6%, 29/471 in primary tumors, $P < 0.0001$, Fisher exact test). Overall, amplifications and losses at baseline or C2D1 compared with EOT within the matched pairs were comparable. Only a small number SCNA were acquired at the EOT. As an example, one patient (Patient 4) acquired losses of *CDKN2A* and *CDKN2B* (genes that encode the cell-cycle inhibitors P16 and P15, respectively, and are both in the same region in 9p).

We next assessed additional genomic features, including TMB (42, 43) and mutational signatures (44, 45) in the 30 ctDNA WES with sufficient TF. These features are associated with breast cancer outcomes and could potentially predict sensitivity or resistance to bazedoxifene plus palbociclib. The median TMBs at baseline ($n = 12$) and EOT ($n = 9$) were comparable and low [baseline median of 1.3 mutations/Mb, range (0.74–19.5); EOT median of 0.87 mutations/Mb, range (0.73–12.0); Wilcoxon $P = 0.84$] (**Fig. 3B**) and there was no significant difference in the TMB in patients who had a clinical benefit compared with patients who did not across all timepoints (Wilcoxon $P = 0.7$).

As for the mutational signatures in the cohort (**Fig. 3C**), the most common mutational signatures (SBS1, SBS5, and SBS40) can be attributed to clock-like and aging processes. The patients with a high TMB (Patient 2, 10, and 30) had enriched APOBEC signatures (SBS2 and SBS13). The same set of APOBEC signatures was detected in patients 21 and 31. Overall, most of the patients with APOBEC signatures (4 of 5 patients) did not have a clinical benefit from bazedoxifene and palbociclib. Albeit a small number of patients, these results are consistent with previous studies showing that the APOBEC signature is associated with endocrine resistance (44) and a high TMB (46). We also detected the mutational signature (SBS17b) that is associated with exposure to chemotherapeutic agents, 5-fluorouracil and capecitabine in a patient who received treatment with capecitabine followed by eribulin prior to enrollment on the study.

Clonal architecture and subclonal evolution during treatment

To better understand how tumor heterogeneity and the subclonal evolution contribute to treatment resistance, we performed an evolutionary analysis (see Patients and Methods). Seven patients had sufficient ctDNA (cfDNA TF ≥ 0.15) from three timepoints or at baseline and EOT (**Fig. 4A–D**; Supplementary Fig. S6A–S6C). In at least 3 of these patients the clonal evolution helped to shed light on potential mechanisms of treatment resistance. Patients 17 (**Fig. 4A**) and 2 (**Fig. 4B**) had clonal *PIK3CA* and *ESR1* pathogenic mutations. Patient 17 had a subclone with losses of the tumor suppressor genes, *RB1* and *PBRM1*, and the abundance of this subclone increased at the time of disease progression [cancer cell fraction (CCF) of 0.10 at baseline increased to 0.52 at EOT]. Patient 2 had two major subclone branches (light blue and red in **Fig. 4B**). Interestingly, within less than 2 months at the time of disease progression, the subclone with an *ESR1* D538G and an *NF1* truncal mutation increased from a CCF of 0.37 at baseline to 1. Loss of neurofibromin was shown to be a mechanism of treatment resistance in HR^+ breast cancer (47). On the other hand, the second subclone with a *SMAD2*-truncating mutation and VHL missense mutation decreased from a CCF of 0.45 at baseline to 0.02 at EOT and is likely not a key driver of the disease progression.

Patient 1 had rapid disease progression within less than a month and was found to have a clonal pathogenic *RB1* mutation (E54*) at baseline and at EOT (**Fig. 4C**). Although this *RB1* mutation is monoallelic, it has been shown that the loss of even one copy of *Rb1* can lead to genomic instability (48). Patient 1 and patient 5 had clonal *ZFHX3* (zinc finger homeobox 3) mutations (**Fig. 4C** and **D**). In addition, three other patients in our study had nonsilent *ZFHX3* mutations (clonal status could not be evaluated in these other patients), making *ZFHX3* a common mutation in our dataset [16% (5/31)]. In contrast, *ZFHX3* mutations, mainly deletions and truncating mutations, were found in only 4% of the ER^+ breast cancers in TCGA cohort (39–41).

Discussion

We provide the first study report of the clinical efficacy and safety of bazedoxifene in combination with palbociclib for the treatment of endocrine-resistant $HR^+/HER2^-$ advanced breast cancer. We observed SD as the best response in 56% of the ITT patient population and 57% in the evaluable patient population. The CBR ≥ 24 weeks was 33% and 34% in the ITT and the evaluable patients, respectively, in a heavily pretreated patient population. The CBR at 24 weeks exceeded the predefined threshold, meeting the primary endpoint of the study.

In this study, >50% of the patients had prior chemotherapy in the metastatic setting, and >40% of the patients had at least two prior lines of ET. Prior chemotherapy is associated with decreased benefit from subsequent treatments (49, 50). In addition, most of the patients had liver metastases, which is also associated with worse outcomes in HR^+ advanced breast cancer (51). Importantly, the results of this study compare favorably to a phase II study of palbociclib as monotherapy in patients with HR^+ advanced breast cancer, in which the CBR ≥ 24 weeks was 21% (7/33; ref. 5), providing evidence for the clinical efficacy of bazedoxifene in this setting.

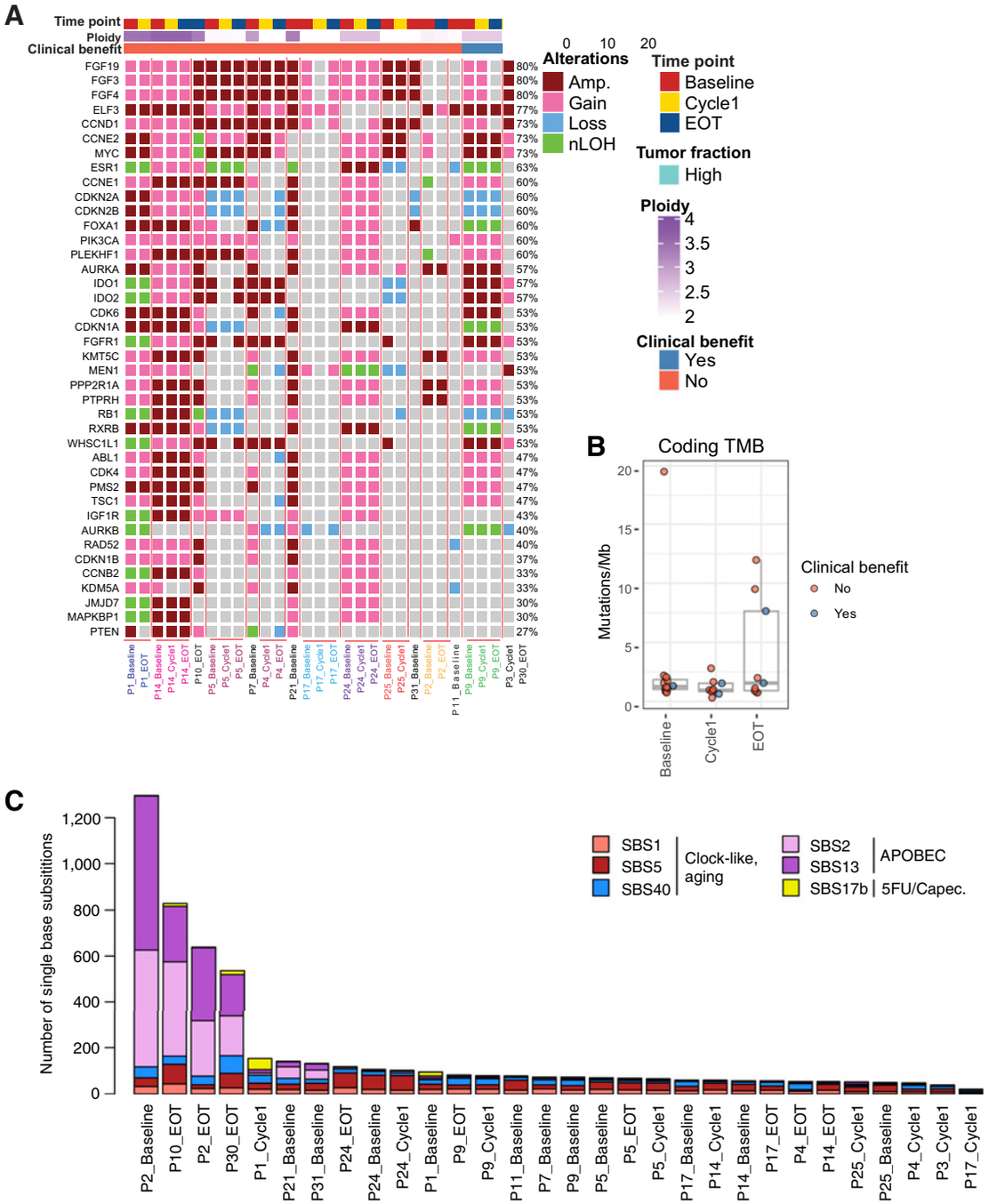

Figure 3.

Copy-number variations, TMB, and mutational signatures. **A,** Somatic copy-number variations [amplifications (AMP), gains, loss, and neutral loss of heterozygosity] in cancer-related genes detected in at least 2 patients. Samples are from 16 patients and include matched samples from at least two timepoints (baseline, C2D1, and EOT) in 9 patients. **B,** Serial TMB at baseline ($n = 28$), C2D1 ($n = 18$), and EOT ($n = 22$). **C,** Mutational signatures detected in cfDNA samples. cfDNA, cell-free DNA.

The need for new ETs when combined with a CDK4/6i that better target the ER mutations in advanced breast cancer is supported by the recent results from the PADA-1 clinical trial. In PADA-1, switching from an AI plus palbociclib to fulvestrant plus palbociclib in patients with HR^+ advanced breast cancer and rising levels of ctDNA *ESR1* mutations, resulted in improved PFS (9). In retrospective analyses, the presence of an *ESR1* mutation did not lead to inferior outcomes with the combination of fulvestrant and a CDK4/6i (52). However, preclinical studies (53) and clinical studies (54, 55) showed decreased activity of single-agent fulvestrant in the presence of the *ESR1*

Figure 4.

Evolutionary analysis of longitudinal plasma ctDNA samples. **A–D,** Left panel showing the phylogenetic trees representing the clonal architecture in plasma ctDNA samples. The number of somatic alterations assigned to each clone and detected alterations in known cancer genes are denoted in each branch. *Truncating mutations. **A–D,** Right panel showing the estimated CCF of each clone at baseline, after 1 cycle of treatment (C2D1) and EOT. The color of the clone matches the respective clone in the phylogenetic trees. ctDNA, circulating tumor DNA.

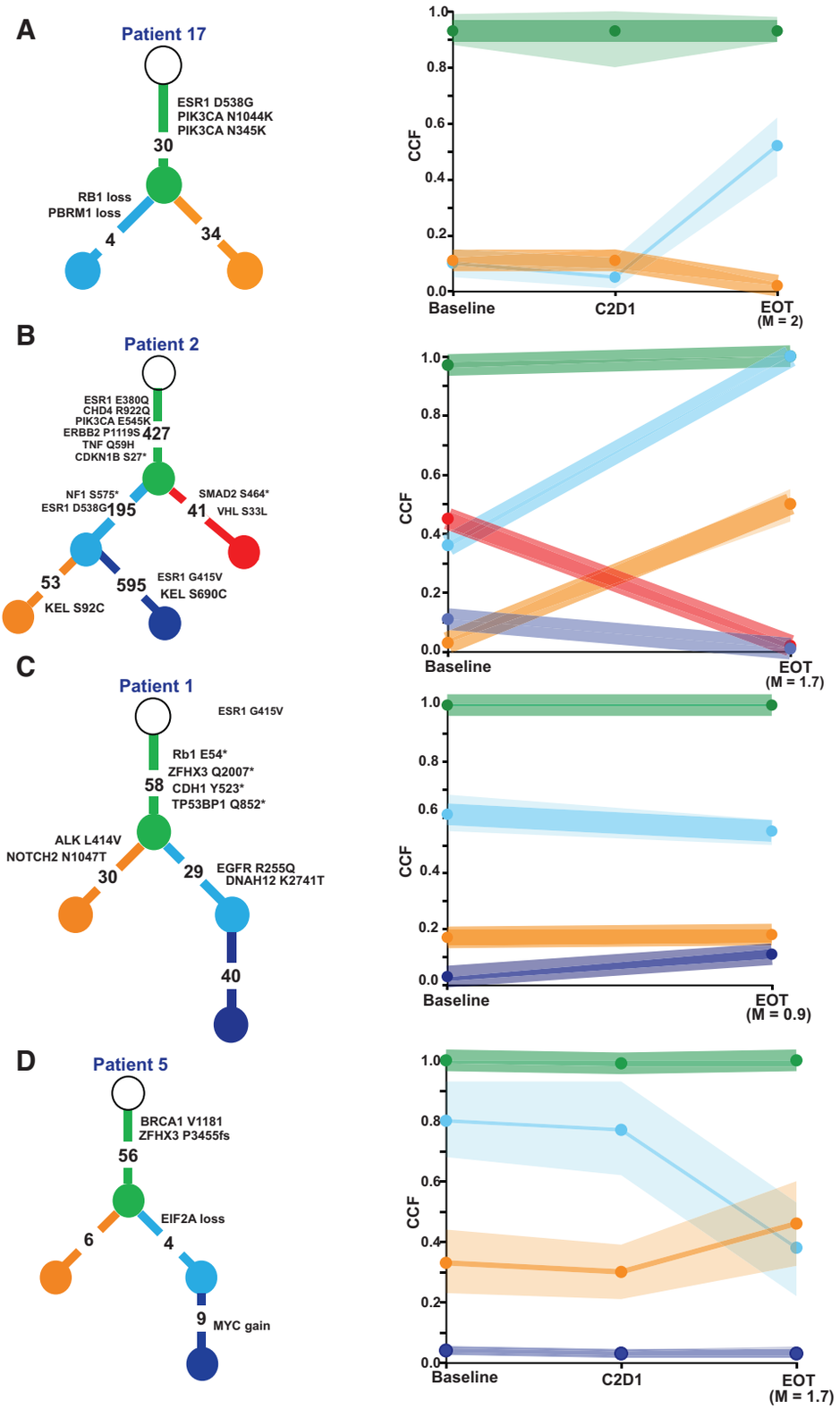

mutations, particularly the Y537S ER mutation. On the other hand, preclinical studies showed that bazedoxifene has superior activity in inhibiting the Y537S ER mutation compared with fulvestrant and biophysical and structural studies provided mechanistic insights explaining these differences (13, 18). In line with these preclinical studies, our clinical trial showed that the presence of an *ESR1* mutation was not associated with decreased benefit from the combination of bazedoxifene and palbociclib. Taken together, these published clinical and preclinical studies, along with the results from our clinical trial support a future randomized clinical trial comparing the combination bazedoxifene plus a CDK4/6i versus fulvestrant plus a CDK4/6i in patients with advanced breast cancer who have rising levels of ctDNA *ESR1* mutations.

The EMERALD trial was a randomized phase III study investigating the new a SSH, elacetsrant, versus standard-of-care ET (AI or fulvestrant; ref. 56). In this trial, patients with HR^+ advanced breast cancer who progressed on prior treatment with ET and a CDK4/6i and were randomized to receive elacestrant had improved PFS compared with patients that received standard-of-care ET. The magnitude of this improvement was higher in patients that had an *ESR1* mutation. These results provided evidence for improved clinical outcomes with a single-agent next-generation ET, particularly in patients that have disease that remains ER dependent and support further development of this class of drugs. However, the median PFS was limited in the EMERALD trial and future studies will need to identify the patients who continue to benefit from ET after treatment with CDK4/6i and investigate novel treatment combination that incorporate the next-generation ETs. Increasing the dose of ET is another potential strategy to improve efficacy from ET, especially in the presence of the Y537S ER mutation, which is characterized by decreased affinity to multiple SERMs and SERDS (19, 57). Because bazedoxifene was well tolerated in large clinical trials with healthy women and in our study in advanced breast cancer, there were no significant gastrointestinal or other DLTs, a trial to investigate the pharmacokinetics, safety, and efficacy of higher doses of bazedoxifene in patients with HR^+ advanced breast cancer and an *ESR1* mutation is warranted.

We performed a prospective analysis of serial ctDNA WES to search for genetic determinants of sensitivity and resistance to the combination of bazedoxifene and palbociclib in advanced breast cancer after multiple lines of treatment. We showed that pathogenic *PIK3CA* mutations were associated with decreased PFS. Preclinical studies support the role of the PI3-kinase pathway in endocrine resistance (58, 59), and the α-specific PI3-kinase inhibitor alpelisib in combination with fulvestrant is approved for the treatment of *PIK3CA*-mutant HR^+ metastatic breast cancer (60). A preclinical study showed that inhibition of PI3 kinase can prevent adaptive resistance to palbociclib, suggesting that the activation of the PI3-kinase pathway is involved in resistance to palbociclib (61). In the phase III PALOMA-III trial in which patients were randomized to fulvestrant plus palbociclib or fulvestrant plus placebo, there was an enrichment of plasma ctDNA *PIK3CA* mutations at the EOT. However, baseline plasma ctDNA *PIK3CA* mutations were not predictive of decreased PFS (10, 62). Our results suggest that in HR^+ advanced breast cancer, the pathogenicity of the *PIK3CA* mutations increases in more advanced metastatic disease after multiple lines of treatment. This is in keeping with previous studies that showed that in metastatic disease, the presence of a *PIK3CA* mutation is associated with treatment resistance and tumor progression (63), whereas in early-stage, treatment-naïve HR^+ breast cancer, *PIK3CA* mutations are associated with improved outcomes (64, 65).

The ctDNA WES analyses also identified genetic alterations that are potential novel drivers of disease progression and treatment resistance. As an example, we identified a high rate of *ELF3* SCNAs. *ELF3* is a member of the ETS transcription factors and is located within 1q32, a region commonly gained in breast cancer. In preclinical studies, ELF3 was shown to be a transcriptional repressor of ER, suggesting a possible role in endocrine resistance (66). We also identified a relatively high rate of *ZFHX3* mutations. *ZFHX3* encodes the transcription factor AT-motif binding factor-1 (ATBF1), which has key roles in protein–protein interactions and is a tumor suppressor in prostate cancer (67). In HR^+ breast cancer, ATBF1 inhibits ER-mediated transcription (68), implying that aberrations in this gene may have a role in resistance to ET.

We acknowledge several limitations in our study, including the small number of patients that limits our ability to make strong conclusions about the efficacy of the combination of bazedoxfene and palbociclib, and the determinants of sensitivity or resistance. In addition, not all the plasma samples had sufficient ctDNA TF for TMB, SCNV, mutational signature, and phylogenetic analyses. Nonetheless, herein we demonstrate the utility and breadth of data that can be gleaned from WES of ctDNA. In summary, our results showed: (i) the safety of bazedoxifene in combination with palbociclib; (ii) a signal of the efficacy of bazedoxifene in HR^+ breast cancer; (iii) *PIK3CA* mutations are a candidate biomarker of resistance to this combination that can be applicable to other next-generation ETs; and (iv) the advantages of WES of ctDNA that enabled us to capture the tumor heterogeneity and subclonal evolution during disease progression. WES also allowed us to identify potential novel genomic mechanisms of tumor progression that warrant future investigation.

Authors' Disclosures

I. Leshchiner reports personal fees and nonfinancial support from ennov1, LLC, and NoRD Bio, Inc and personal fees from PACT Pharma, Inc. outside the submitted work. S.M. Tolaney reports grants and personal fees from Pfizer during the conduct of the study as well as grants and personal fees from AstraZeneca, Merck, Genentech/Roche, Novartis, SeaGen, Eli Lilly, Gilead, Bristol-Myers Squibb, Eisai, and Sanofi; grants from Exelixis, Nektar, Cyclacel, and NanoString; and personal fees from Daiichi Sankyo, Athenex, CytomX, Certara, Mersana Therapeutics, Ellipses Pharma, 4D Pharma, Infinity Therapeutics, OncoSec Medical Inc, Chugai Pharmaceuticals, BeyondSpring Pharmaceuticals, OncXerna, Zymeworks, Zentalis, Blueprint Medicines, Reveal Genomics, ARC Therapeutics, Myovant, Umoja Buopharma, and Menarini/Stemline outside the submitted work. D.P. McDonnell reports personal fees from Pfizer and grants from NIH during the conduct of the study as well as grants, personal fees, and other support from Zentalis Pharmaceuticals and RAPPTA Therapeutics; other support from G1 Therapeutics and XRAD Therapeutics; and grants and personal fees from BMS outside the submitted work. In addition, D.P. McDonnell has a patent for a method of treating cancer using selective estrogen receptor modulators (US10,071,066, US10,420,734 issued, licensed, and with royalties paid from Radius Health) and a patent for lasofoxifene for treatment of breast cancer (US10,258,604, US10,905659, issued, licensed, and with royalties paid from Sermonix). I.E. Krop reports personal fees from AstraZeneca, Daiichi Sankyo, Genentech/Roche, Novartis, Merck, and Macrogenics and grants from Genentech/Roche and Pfizer outside the submitted work. E.P. Winer reports grants from Maor Foundation during the conduct of the study as well as other support from Carrick Therapeutics, Genentech/Roche, Jounce Therapeutics, and Leap Therapeutics outside the submitted work. G. Getz reports personal fees from Scorpion Therapeutics and grants from IBM during the conduct of the study as well as grants from Pharmacyclics outside the submitted work; in addition, G Getz is an inventor on patent applications related to MSMuTect, MSMutSig, MSIDetect, Polysolver, and SignatureAnalyzer-GPU and is a founder of, is a consultant for, and holds privately equity in Scorpion Therapeutics. R. Jeselsohn reports grants from Pfizer during the conduct of the study as well as grants from Lilly and personal fees from GE Healthcare outside the submitted work. No disclosures were reported by the other authors.

Authors' Contributions

J. Tsuji: Formal analysis, investigation, methodology, writing–original draft, writing–review and editing. **T. Li:** Formal analysis, visualization, methodology, writing–original draft, writing–review and editing. **A. Grinshpun:** Data curation, investigation, visualization, writing–review and editing. **T. Coorens:** Formal analysis, visualization, writing–original draft, writing–review and editing. **D. Russo:** Formal analysis, visualization, writing–original draft, writing–review and editing. **L. Anderson:** Data curation, project administration, writing–review and editing. **R. Rees:** Data curation, writing–review and editing. **A. Nardone:** Data curation, writing–review and editing. **C. Patterson:** Data curation, project administration, writing–review and editing. **N.J. Lennon:** Supervision, writing–review and editing. **C. Cibulskis:** Supervision, writing–review and editing. **I. Leshchiner:** Formal analysis, writing–review and editing. **N. Tayob:** Formal analysis, supervision, validation, writing–review and editing. **S.M. Tolaney:** Supervision, writing–review and editing. **N. Tung:** Supervision, investigation, writing–review and editing. **D.P. McDonnell:** Conceptualization, investigation, writing–review and editing. **I.E. Krop:** Conceptualization, supervision, investigation, writing–review and editing. **E.P. Winer:** Conceptualization, supervision, investigation, writing–review and editing. **C. Stewart:** Formal analysis, supervision, writing–original draft, writing–review and editing. **G. Getz:** Conceptualization, supervision, investigation, visualization, methodology, writing–original draft, writing–review and editing. **R. Jeselsohn:** Conceptualization, supervision, funding acquisition, investigation, visualization, writing–original draft, writing–review and editing.

Acknowledgments

The study was conducted with funding from Pfizer. R. Jeselsohn is funded by the Claudia Adams Barr Program and an R01 CA237414-01.

We thank Myles Brown for helpful discussion. We thank Sam Pollock and Fanny Dao for assistance in sequencing data management. G. Getz was partially funded by the Paul C. Zamecnik Chair in Oncology at the Massachusetts General Hospital Cancer Center.

The publication costs of this article were defrayed in part by the payment of publication fees. Therefore, and solely to indicate this fact, this article is hereby marked "advertisement" in accordance with 18 USC section 1734.

Note

Supplementary data for this article are available at Clinical Cancer Research Online (http://clincancerres.aacrjournals.org/).

Received July 25, 2022; revised September 10, 2022; accepted October 6, 2022; published first October 10, 2022.

References

1. Lynce F, Shajahan-Haq AN, Swain SM. CDK4/6 inhibitors in breast cancer therapy: current practice and future opportunities. Pharmacol Ther 2018;191:65–73.
2. Watts CK, Sweeney KJ, Warlters A, Musgrove EA, Sutherland RL. Antiestrogen regulation of cell cycle progression and cyclin D1 gene expression in MCF-7 human breast cancer cells. Breast Cancer Res Treat 1994;31:95–105.
3. Finn RS, Dering J, Conklin D, Kalous O, Cohen DJ, Desai AJ, et al. PD 0332991, a selective cyclin D kinase 4/6 inhibitor, preferentially inhibits proliferation of luminal estrogen receptor-positive human breast cancer cell lines *in vitro*. Breast Cancer Res 2009;11:R77.
4. Eeckhoute J, Carroll JS, Geistlinger TR, Torres-Arzayus MI, Brown M. A cell-type-specific transcriptional network required for estrogen regulation of cyclin D1 and cell cycle progression in breast cancer. Genes Dev 2006;20:2513–26.
5. DeMichele A, Clark AS, Tan KS, Heitjan DF, Gramlich K, Gallagher M, et al. CDK 4/6 inhibitor palbociclib (PD0332991) in Rb+ advanced breast cancer: phase II activity, safety, and predictive biomarker assessment. Clin Cancer Res 2015;21:995–1001.
6. Formisano L, Stauffer KM, Young CD, Bhola NE, Guerrero-Zotano AL, Jansen VM, et al. Association of FGFR1 with ERalpha maintains ligand-independent ER transcription and mediates resistance to estrogen deprivation in ER(+) breast cancer. Clin Cancer Res 2017;23:6138–50.
7. Formisano L, Lu Y, Servetto A, Hanker AB, Jansen VM, Bauer JA, et al. Aberrant FGFR signaling mediates resistance to CDK4/6 inhibitors in ER+ breast cancer. Nat Commun 2019;10:1373.
8. Bidard FC, Callens C, Dalenc F, Pistilli B, Rouge T, Clatot F, et al. Prognostic impact of ESR1 mutations in ER+ HER2- MBC patients prior treated with first line AI and palbociclib: an exploratory analysis of the PADA-1 trial. J Clin Oncol 38: 15s, 2020 (suppl; abstr 1010).
9. Jacobson A. Early switch to fulvestrant plus palbociclib improves outcomes in esr1-mutated, estrogen receptor-positive metastatic breast cancer. Oncologist 2022;27:S9–S10.
10. O'Leary B, Cutts RJ, Liu Y, Hrebien S, Huang X, Fenwick K, et al. The genetic landscape and clonal evolution of breast cancer resistance to palbociclib plus fulvestrant in the PALOMA-3 Trial. Cancer Discov 2018;8:1390–403.
11. Wardell SE, Nelson ER, Chao CA, McDonnell DP. Bazedoxifene exhibits antiestrogenic activity in animal models of tamoxifen-resistant breast cancer: implications for treatment of advanced disease. Clin Cancer Res 2013;19:2420–31.
12. Lewis-Wambi JS, Kim H, Curpan R, Grigg R, Sarker MA, Jordan VC. The selective estrogen receptor modulator bazedoxifene inhibits hormone-independent breast cancer cell growth and down-regulates estrogen receptor alpha and cyclin D1. Mol Pharmacol 2011;80:610–20.
13. Fanning SW, Jeselsohn R, Dharmarajan V, Mayne CG, Karimi M, Buchwalter G, et al. The SERM/SERD bazedoxifene disrupts ESR1 helix 12 to overcome acquired hormone resistance in breast cancer cells. Elife 2018;7:e37161.
14. Peng L, Luo Q, Lu H. Efficacy and safety of bazedoxifene in postmenopausal women with osteoporosis: a systematic review and meta-analysis. Medicine 2017;96:e8659.
15. Mirkin S, Archer DF, Taylor HS, Pickar JH, Komm BS. Differential effects of menopausal therapies on the endometrium. Menopause 2014;21:899–908.
16. Duggan ST, McKeage K. Bazedoxifene: a review of its use in the treatment of postmenopausal osteoporosis. Drugs 2011;71:2193–212.
17. Song Y, Santen RJ, Wang JP, Yue W. Inhibitory effects of a bazedoxifene/conjugated equine estrogen combination on human breast cancer cells *in vitro*. Endocrinology 2013;154:656–65.
18. Wardell SE, Ellis MJ, Alley HM, Eisele K, VanArsdale T, Dann SG, et al. Efficacy of SERD/SERM Hybrid-CDK4/6 inhibitor combinations in models of endocrine therapy-resistant breast cancer. Clin Cancer Res 2015;21:5121–30.
19. Hosfield DJ, Weber S, Li NS, Sauvage M, Joiner CF, Hancock GR, et al. Stereospecific lasofoxifene derivatives reveal the interplay between estrogen receptor alpha stability and antagonistic activity in ESR1 mutant breast cancer cells. Elife 2022;11:e72512.
20. Press MF, Seoane JA, Curtis C, Quinaux E, Guzman R, Sauter G, et al. Assessment of ERBB2/HER2 status in HER2-equivocal breast cancers by FISH and 2013/2014 ASCO-CAP Guidelines. JAMA Oncol 2019;5:366–75.
21. Eisenhauer EA, Therasse P, Bogaerts J, Schwartz LH, Sargent D, Ford R, et al. New response evaluation criteria in solid tumours: revised RECIST guideline (version 1.1). Eur J Cancer 2009;45:228–47.
22. Costelloe CM, Chuang HH, Madewell JE, Ueno NT. Cancer response criteria and bone metastases: RECIST 1.1, MDA and PERCIST. J Cancer 2010;1:80–92.
23. Christiansen C, Chesnut CH 3rd, Adachi JD, Brown JP, Fernandes CE, Kung AW, et al. Safety of bazedoxifene in a randomized, double-blind, placebo- and active-controlled Phase 3 study of postmenopausal women with osteoporosis. BMC Musculoskelet Disord 2010;11:130.
24. Adalsteinsson VA, Ha G, Freeman SS, Choudhury AD, Stover DG, Parsons HA, et al. Scalable whole-exome sequencing of cell-free DNA reveals high concordance with metastatic tumors. Nat Commun 2017;8:1324.
25. Taylor-Weiner A, Stewart C, Giordano T, Miller M, Rosenberg M, Macbeth A, et al. DeTiN: overcoming tumor-in-normal contamination. Nat Methods 2018;15:531–4.
26. Cibulskis K, McKenna A, Fennell T, Banks E, DePristo M, Getz G. ContEst: estimating cross-contamination of human samples in next-generation sequencing data. Bioinformatics 2011;27:2601–2.
27. Cibulskis K, Lawrence MS, Carter SL, Sivachenko A, Jaffe D, Sougnez C, et al. Sensitive detection of somatic point mutations in impure and heterogeneous cancer samples. Nat Biotechnol 2013;31:213–9.

28. Kim S, Scheffler K, Halpern AL, Bekritsky MA, Noh E, Kallberg M, et al. Strelka2: fast and accurate calling of germline and somatic variants. Nat Methods 2018;15: 591–4.
29. Karczewski KJ, Francioli LC, Tiao G, Cummings BB, Alfoldi J, Wang Q, et al. The mutational constraint spectrum quantified from variation in 141,456 humans. Nature 2020;581:434–43.
30. Chakravarty D, Gao J, Phillips SM, Kundra R, Zhang H, Wang J, et al. OncoKB: a precision oncology knowledge base. JCO Precis Oncol 2017;2017:PO.17.00011.
31. Kim J, Mouw KW, Polak P, Braunstein LZ, Kamburov A, Kwiatkowski DJ, et al. Somatic ERCC2 mutations are associated with a distinct genomic signature in urothelial tumors. Nat Genet 2016;48:600–6.
32. Gori K, Baez-Ortega A. sigfit: flexible Bayesian inference of mutational signatures. bioRxiv 2020:372896.
33. Carter SL, Cibulskis K, Helman E, McKenna A, Shen H, Zack T, et al. Absolute quantification of somatic DNA alterations in human cancer. Nat Biotechnol 2012;30:413–21.
34. Leshchiner I, Livitz D, Gainor JF, Rosebrock D, Spiro O, Martinez A, et al. Comprehensive analysis of tumour initiation, spatial and temporal progression under multiple lines of treatment. bioRxiv 2019:508127.
35. Bielski CM, Zehir A, Penson AV, Donoghue MTA, Chatila W, Armenia J, et al. Genome doubling shapes the evolution and prognosis of advanced cancers. Nat Genet 2018;50:1189–95.
36. Hanker AB, Sudhan DR, Arteaga CL. Overcoming endocrine resistance in breast cancer. Cancer Cell 2020;37:496–513.
37. Wander SA, Cohen O, Gong X, Johnson GN, Buendia-Buendia JE, Lloyd MR, et al. The genomic landscape of intrinsic and acquired resistance to cyclin-dependent kinase 4/6 inhibitors in patients with hormone receptor-positive metastatic breast cancer. Cancer Discov 2020;10:1174–93.
38. Cornell L, Wander SA, Visal T, Wagle N, Shapiro GI. MicroRNA-mediated suppression of the TGF-beta pathway confers transmissible and reversible CDK4/6 inhibitor resistance. Cell Rep 2019;26:2667–80.
39. Cerami E, Gao J, Dogrusoz U, Gross BE, Sumer SO, Aksoy BA, et al. The cBio cancer genomics portal: an open platform for exploring multidimensional cancer genomics data. Cancer Discov 2012;2:401–4.
40. Gao J, Aksoy BA, Dogrusoz U, Dresdner G, Gross B, Sumer SO, et al. Integrative analysis of complex cancer genomics and clinical profiles using the cBioPortal. Sci Signal 2013;6:pl1.
41. Koboldt DC, Fulton RS, McLellan MD, Schmidt H, Kalicki-Veizer J, McMichael JF, et al. Comprehensive molecular portraits of human breast tumours. Nature 2012;490:61–70.
42. van Geelen CT, Savas P, Teo ZL, Luen SJ, Weng CF, Ko YA, et al. Clinical implications of prospective genomic profiling of metastatic breast cancer patients. Breast Cancer Res 2020;22:91.
43. Aftimos P, Oliveira M, Irrthum A, Fumagalli D, Sotiriou C, Gal-Yam EN, et al. Genomic and transcriptomic analyses of breast cancer primaries and matched metastases in AURORA, the breast international group (BIG) molecular screening initiative. Cancer Discov 2021;11:2796–811.
44. Law EK, Sieuwerts AM, LaPara K, Leonard B, Starrett GJ, Molan AM, et al. The DNA cytosine deaminase APOBEC3B promotes tamoxifen resistance in ER-positive breast cancer. Sci Adv 2016;2:e1601737.
45. Bertucci F, Ng CKY, Patsouris A, Droin N, Piscuoglio S, Carbuccia N, et al. Genomic characterization of metastatic breast cancers. Nature 2019;569:560–4.
46. Barroso-Sousa R, Jain E, Cohen O, Kim D, Buendia-Buendia J, Winer E, et al. Prevalence and mutational determinants of high tumor mutation burden in breast cancer. Ann Oncol 2020;31:387–94.
47. Zheng ZY, Anurag M, Lei JT, Cao J, Singh P, Peng J, et al. Neurofibromin is an estrogen receptor-alpha transcriptional co-repressor in breast cancer. Cancer Cell 2020;37:387–402.
48. Coschi CH, Ishak CA, Gallo D, Marshall A, Talluri S, Wang J, et al. Haploin-sufficiency of an RB-E2F1-Condensin II complex leads to aberrant replication and aneuploidy. Cancer Discov 2014;4:840–53.
49. Roche H, Vahdat LT. Treatment of metastatic breast cancer: second line and beyond. Ann Oncol 2011;22:1000–10.
50. Park IH, Lee KS, Ro J. Effects of second and subsequent lines of chemotherapy for metastatic breast cancer. Clin Breast Cancer 2015;15:e55–62.
51. Robertson JFR, Di Leo A, Johnston S, Chia S, Bliss JM, Paridaens RJ, et al. Meta-analyses of visceral versus non-visceral metastatic hormone receptor-positive breast cancer treated by endocrine monotherapies. NPJ Breast Cancer 2021;7:11.
52. Fribbens C, O'Leary B, Kilburn L, Hrebien S, Garcia-Murillas I, Beaney M, et al. Plasma ESR1 mutations and the treatment of estrogen receptor-positive advanced breast cancer. J Clin Oncol 2016;34:2961–8.
53. Jeselsohn R, Yelensky R, Buchwalter G, Frampton G, Meric-Bernstam F, Gonzalez-Angulo AM, et al. Emergence of constitutively active estrogen receptor-alpha mutations in pretreated advanced estrogen receptor-positive breast cancer. Clin Cancer Res 2014;20:1757–67.
54. O'Leary B, Hrebien S, Morden JP, Beaney M, Fribbens C, Huang X, et al. Early circulating tumor DNA dynamics and clonal selection with palbociclib and fulvestrant for breast cancer. Nat Commun 2018;9:896.
55. Tolaney SM, Toi M, Neven P, Sohn J, Grischke EM, Llombart-Cussac A, et al. Clinical significance of PIK3CA and ESR1 mutations in circulating tumor DNA: analysis from the MONARCH 2 study of abemaciclib plus fulvestrant. Clin Cancer Res 2022;28:1500–6.
56. Bidard FC, Kaklamani VG, Neven P, Streich G, Montero AJ, Forget F, et al. Elacestrant (oral selective estrogen receptor degrader) versus standard endocrine therapy for estrogen receptor-positive, human epidermal growth factor receptor 2-negative advanced breast cancer: results from the randomized phase III EMERALD trial. J Clin Oncol 2022;40:3246–56.
57. Fanning SW, Mayne CG, Dharmarajan V, Carlson KE, Martin TA, Novick SJ, et al. Estrogen receptor alpha somatic mutations Y537S and D538G confer breast cancer endocrine resistance by stabilizing the activating function-2 binding conformation. Elife 2016;5:e12792.
58. Campbell RA, Bhat-Nakshatri P, Patel NM, Constantinidou D, Ali S, Nakshatri H. Phosphatidylinositol 3-kinase/AKT-mediated activation of estrogen receptor alpha: a new model for anti-estrogen resistance. J Biol Chem 2001;276:9817–24.
59. Ma CX, Crowder RJ, Ellis MJ. Importance of PI3-kinase pathway in response/resistance to aromatase inhibitors. Steroids 2011;76:750–2.
60. Andre F, Ciruelos E, Rubovszky G, Campone M, Loibl S, Rugo HS, et al. Alpelisib for PIK3CA-mutated, hormone receptor-positive advanced breast cancer. N Engl J Med 2019;380:1929–40.
61. Herrera-Abreu MT, Palafox M, Asghar U, Rivas MA, Cutts RJ, Garcia-Murillas I, et al. Early adaptation and acquired resistance to CDK4/6 inhibition in estrogen receptor-positive breast cancer. Cancer Res 2016;76:2301–13.
62. Tolaney SM, Toi M, Neven P, Sohn J, Grischke EM, Llombart-Cussac A, et al. Clinical significance of PIK3CA and ESR1 mutations in circulating tumor DNA: analysis from the MONARCH 2 study of abemaciclib plus fulvestrant. Clin Cancer Res 2022;28:1500–6.
63. Mosele F, Stefanovska B, Lusque A, Tran Dien A, Garberis I, Droin N, et al. Outcome and molecular landscape of patients with PIK3CA-mutated metastatic breast cancer. Ann Oncol 2020;31:377–86.
64. Kalinsky K, Jacks LM, Heguy A, Patil S, Drobnjak M, Bhanot UK, et al. PIK3CA mutation associates with improved outcome in breast cancer. Clin Cancer Res 2009;15:5049–59.
65. Zardavas D, Te Marvelde L, Milne RL, Fumagalli D, Fountzilas G, Kotoula V, et al. Tumor PIK3CA genotype and prognosis in early-stage breast cancer: a pooled analysis of individual patient data. J Clin Oncol 2018;36:981–90.
66. Gajulapalli VN, Samanthapudi VS, Pulaganti M, Khumukcham SS, Malisetty VL, Guruprasad L, et al. A transcriptional repressive role for epithelial-specific ETS factor ELF3 on oestrogen receptor alpha in breast cancer cells. Biochem J 2016; 473:1047–61.
67. Sun X, Frierson HF, Chen C, Li C, Ran Q, Otto KB, et al. Frequent somatic mutations of the transcription factor ATBF1 in human prostate cancer. Nat Genet 2005;37:407–12.
68. Dong XY, Sun X, Guo P, Li Q, Sasahara M, Ishii Y, et al. ATBF1 inhibits estrogen receptor (ER) function by selectively competing with AIB1 for binding to the ER in ER-positive breast cancer cells. J Biol Chem 2010;285:32801–9.